Detecting the Effects of Variant STING Agonist Administration on Dendritic Cell Endosomal pH Using the Ratiometric Method

Omeed Yazdani

A thesis

submitted in partial fulfillment of the

requirements for the degree of

Master of Science

University of Washington

2025

Committee:

Suzie Hwang Pun

Christopher Neils

Program Authorized to Offer Degree:

Bioengineering

University of Washington

Abstract

Detecting the Effects of Variant STING Agonist Administration on Dendritic Cell Endosomal pH Using the Ratiometric Method

Omeed Yazdani

Chair of the Supervisory Committee:

Suzie Hwang Pun

Department of Bioengineering

Peptide cancer vaccines have had limited clinical success despite their safety, characterization, and production advantages. We hypothesize that the poor immunogenicity of peptides can be surmounted by delivery vehicles that overcome the systemic and cellular drug delivery barriers faced by peptides. We introduce polySTING and NPSTING, copolymerized, mannosylated variants of the STING-3 agonist known to activate the cGAS-STING signaling pathway, promoting the release of type-1 interferons and pro-inflammatory cytokines leading to effective tumor immunogenicity. The STING-3 agonist is a non-nucleotide molecule that successfully activates the STING pathway, but it has poor solubility, which limits its usage in vivo. The developed poly-STING platform improves the drug's solubility and provides enzyme-triggered drug release upon delivery, which has been shown to induce improved therapeutic efficacy compared to the free STING-3 agonist. The Pun lab seeks to investigate modalities for optimization

of the cGAS-STING pathway activation through investigating effects caused by mannosylation of the polymer. Dendritic cells (DCs) are crucial for initiating cytotoxic T-cell responses through antigen presentation via the MHC class-I pathway. The cGAS-STING signaling pathway enhances DC maturation and antigen cross-presentation but may interfere with pH-dependent antigen release systems such as the VIPER nanocarrier. This thesis investigates whether STING agonist variants alter DC endosomal pH, potentially affecting VIPER-mediated antigen escape. A ratiometric assay using FITC and Alexa Fluor 647-conjugated dextrans was developed and optimized for flow cytometry-based endosomal pH measurement. Protocol refinements—such as transitioning to a 96-well plate format and implementing valinomycin/nigericin permeabilization—enabled robust, high-throughput analysis with improved cell viability. Results confirmed biologically relevant endosomal acidification profiles over time in DCs. Experimentation showed that co-treatment with STING variants does not drastically alter the acidification trend when compared to PBS, but rather there is a slight delayed acidification. This implies that STING activation effects on endosomal pH might require time to become apparent. A 30-minute pretreatment experiment showed minor delayed acidification in experimental groups compared to PBS, with PolySTING being the most drastic. This assay lays the groundwork for evaluating how variant STING agonists, particularly polySTING and NPSTING, modulate endosomal pH and thereby influence antigen release and immune activation, guiding the design of more effective cancer vaccine delivery platforms.

Introduction

Medical Motivation for the Project and the Statement of the Problem to be Addressed

Cancer encompasses a broad range of diseases characterized by abnormal cells that have lost cell cycle control and thus divide uncontrollably, spread throughout the body, and destroy normally functioning body tissue. According to the American Cancer Society, there will be an estimated 1.9 million new cancer cases diagnosed in the US alone this year, with over $200 billion being spent nationwide on treatment alone. Additionally, there will be about 600,000 new deaths accompanying the diagnoses, with this frightening number only getting larger [1 - 2]. Therefore, it is imperative that preventative measures that can be taken against cancer are found soon in order to stabilize these large numbers. The rise of immunotherapy in recent years has started the largest paradigm shift in cancer treatment since the development of chemotherapies in the 1940s. Instead of targeting malignant cells, cancer immunotherapies coordinate with the host immune system to combat tumors. The major types of immunotherapy include immune checkpoint inhibitors, monoclonal antibodies, T-cell therapies, and vaccines. Cancer vaccines, which teach the immune system to recognize and remove tumor cells, offer the possibility of eliciting highly tumor-specific responses that provide sustained protection against recurrence. As a result, cancer subunit vaccines have recently been sought after as extremely viable ways of training one's immune system to recognize and attack these cancerous tumor cells using tumor antigen structural motifs. This is because they generally garner improved safety when compared to whole antigens, a low manufacturing cost, ease of synthesis, and increased shelf stability [3]. Yet despite these notable characteristics, peptide antigen vaccines have seen low clinical efficacy in an oncological context due to poor immunogenicity [4].

Cytotoxic T-cells are known to have very effective tumor-eradicating responses, but a large part of priming these cells is antigen presentation through the major histocompatibility complex (MHC) class-I pathway and eliciting a tumor-infiltrating response. As a result, equipping the vaccine with some sort of access to these pathways is important and, in fact, necessary for the vaccine to induce effective tumor clearance. The most common way of inducing the MHC class-I pathway is through dendritic cell (DC) maturation and activation, which then activates cytotoxic T-cells and natural killer cells. These cells then recognize tumor-associated antigens and act accordingly, killing the tumor cells via apoptosis. Thus, effective cancer vaccines must replicate and activate various critical aspects leading to tumor eradication, including internalization and recognition of tumor antigens by DCs, activation of these DCs, antigen presentation by MHC I molecules, and priming of adaptive T cell immunity against tumors.

As stated above, peptide antigen vaccines have seen a large increase in popularity recently due to their ease of production on a large scale and long-term storage stability. These advantages will allow immunotherapies to be widely available all over the world, regardless of socioeconomic status. Unfortunately, peptide antigens are known to be very poorly immunogenic and have low bioactivity due to degradation. As a

result, antigens need some sort of carrier motif to provide stabilization and increased targeting potential while simultaneously protecting against in vivo degradation of the agonist and/or adjuvant.

A commonly used pathway for priming DCs is the Cyclic GMP-AMP Synthase - Stimulator of Interferon Genes (cGAS-STING) signaling pathway. STING activation in DCs drives antitumor immunity by triggering DC maturation, migration to lymph nodes, and enhanced antigen cross-presentation to CD8+ T cells. While IFN-β production remains critical, the cGAS-STING pathway also activates DCs through IFN-I-independent mechanisms such as autophagy induction and metabolic reprogramming. Current clinical STING agonists like STING-3 face limitations due to poor aqueous solubility (<0.5 mg/mL) and lack of cell-type specificity, leading to systemic toxicity and suboptimal DC activation. To address this, the Pun lab has developed polySTING: a water-soluble copolymer with mannosylated monomers targeting CD206+ DCs and a STING agonist prodrug monomer linked via cathepsin B-cleavable valine-alanine linkers. This design leverages DC-specific mannose receptor expression (CD206) for precise delivery. The NPSTING variant we have developed further enables co-delivery of tumor antigens through pH-triggered nanoparticle assembly, synchronizing antigen presentation with STING-mediated DC maturation. This synchronized antigen presentation and STING activation enhances DC-mediated T cell priming while minimizing off-target effects.

To surmount the delivery challenges associated with DC antigen presentation, the Pun lab has developed a mannosylated virus inspired polymer for endosomal release (Man-VIPER). VIPER is a self-assembling polymer that forms small micelles around 40 nm at physiological pH, making it well-suited for efficient lymph node drainage and uptake by DCs [5]. The platform is mannosylated, which means it displays mannose residues on its surface, allowing it to specifically target the mannose receptor (CD206) highly expressed on DCs. This targeting significantly enhances the delivery of antigens directly to these key antigen-presenting cells, improving the likelihood of a strong immune response.

A central feature of VIPER is its pH-responsive behavior. At neutral pH, VIPER encapsulates both the antigen and a membrane-lytic peptide called melittin in its core, shielding melittin's disruptive activity and minimizing off-target toxicity. Once VIPER is taken up by DCs and trafficked into the acidic environment of the endosome, the polymer undergoes a conformational change that exposes melittin. This exposure allows melittin to disrupt the endosomal membrane, releasing the antigen into the cytosol where it can be efficiently processed for cross-presentation on MHC-I molecules.

By co-delivering the antigen with a STING agonist as an adjuvant, VIPER enables the combination of potent innate immune activation with efficient antigen presentation, which is essential for robust and durable antitumor immunity. However, because VIPER's endosomal escape mechanism is triggered by the acidic pH of the DC endosome, it is important to determine whether STING activation affects this process. To address this, I have developed a protocol to measure endo-lysosomal pH in DCs

over time using both pH-sensitive and pH-agnostic rhodamine dyes conjugated to dextrans. This will allow us to assess pH changes in DC endosomes to determine whether STING will impact VIPER's ability to release antigen into the cytosol, and to optimize our delivery system for combined therapies.

The work done in this project is funded by an R01 grant from the National Institutes of Health. The purpose of R01 grant proposals is to fund research that develops and finds knowledge in line with the NIH's mission to develop resources and knowledge that will enhance human health in a multitude of different ways [6]. My project specifically involves the cure and prevention of cancer, and thus it falls under the NIH's goal to support research in the cure of human disease.

Literature Review

The community of scientists working to develop vaccines for cancer immunotherapy has generally acknowledged the importance of cGAS-STING pathway activation for the downstream release of type-one interferons, which promote maturation and migration of DCs, bridging innate and adaptive immunity. Thus, various recent studies have been done studying the effects of conjugating various groups to the STING agonist and observing any cGAS-STING pathway activation for cancer immunotherapy.

Currently, efforts are focused on designing modified cyclic dinucleotide adjuvants that are similar to the STING ligand cGAMP, and some have even progressed into clinical trials. Specifically, expressing high levels of cyclic-di-AMP has been shown to result in pro-inflammatory cytokine responses, which then indicate activation of the STING pathway. The group that performed these experiments also reported high levels of trained immunity across many other parameters in both murine and human primary cells [7]. On the other hand, one group reported the development of an amidobenzimidizole dimer compound that showed enhanced STING binding [8]. In fact, intravenous injection of their designed homodimeric STING agonist showed complete colon tumor regression that was lasting. At the end of their 43-day tumor reduction study, 8 out of 10 mice presented as completely tumor-free. Another group that reported a 100% survival rate after a 60-day tumor reduction study showed that the combination of a STING agonist with anti-PD-1 antibodies showed great synergistic effects in tumor eradication since T-cells were prevented from "turning off" without their PD-1 checkpoint protein being active [9]. It is important to note though that prolonged immune checkpoint blockade inhibitor treatment can lead to T cell exhaustion in some cases.

Another important part of STING activation for cancer immunotherapy is the activation of tumor-associated macrophages, leading to the phagocytosis of cancer cells by themselves or the recruitment of other important immune cells to eradicate the tumor [10]. Activation of these tumor-associated macrophages via the STING pathway by the commonly used cyclic-di-AMP, cyclic-di-GMP, or cyclic-GMP-AMP shows a very high rate of activated macrophages polarizing from M2 to M1 types in vivo. M1-type macrophages are pro-inflammatory and thus more effective for tumor response, meaning that STING activation does in fact effectively activate macrophages for potent antitumor efficacy [11 - 12]. Because M1-type macrophages are the only

pro-inflammatory type, for optimal immunity, the drug should only target M2-types for repolarization. Many groups show success in this by targeting the CD206 receptor, which is primarily expressed in only M2 macrophages. This has been done by tagging drugs with mannose or mannose-like chemicals, since CD206 is in fact a mannose receptor [13 - 14]. To test for drug uptake and macrophage repolarization, many studies are utilizing RT-qPCR by lysing tumor cells after in vivo inoculation and vaccine introduction, to look for pro-inflammatory chemokine expression and markers for STING activation in macrophages [15 - 16].

Emerging research also highlights that STING activation induces significant pH alterations in key DC organelles, with implications for antigen processing and adjuvant delivery systems. STING functions as a proton channel in human cells, mediating Golgi lumen alkalinization through direct proton efflux during its trafficking from the ER to Golgi compartments [17]. However, the alkalinization of Golgi-derived vesicles may interfere with pH-sensitive drug delivery systems like VIPER nanoparticles, which require acidic endosomal environments for optimal antigen release. These findings underscore the need to characterize STING-mediated pH alterations when designing combination therapies using pH-responsive nanocarriers and STING agonists.

Previous Work by Others

I am incredibly thankful to my collaborators in the Stayton lab for their continual help with working through challenges involving conjugate chemistry and copolymerization. In the past, they had been working to develop drug carriers for targeting alveolar macrophages, using a self-coined "drugamer" platform consisting of copolymerized hydrophilic mannose residues linked to their prodrug consisting of enzyme-cleavable dipeptide or phenyl-ester links for controlled release and dosage. After monomer development, RAFT polymerization was used to copolymerize the prodrug and mannose monomers into a well-defined drugamer [18]. Their previous work with optimizing mannose conjugation to the drug as well as developing methods to incorporate controllable release properties for designated drug dosing can be incorporated into my designed STING activating drug platform to test for and control any cytotoxicity due to drug dosage.

Over the course of this project, the Pun lab has explored how the structural properties of polymeric STING agonists shape therapeutic vaccine efficacy. In particular, a pivotal experiment led by Dr. Kefan Song assessed the antitumor effects of VIPER vaccine formulations adjuvanted with structurally distinct STING drugamers in the aggressive B16-OVA melanoma model. C57BL/6 mice were inoculated with B16-OVA tumor cells on day 0, and vaccinated subcutaneously on days 4, 11, and 18 with either VIPER alone, VIPER plus free STING agonist, VIPER plus polySTING, or VIPER combined with NPSTING—either co-micellized (VIPER-co-NPSTING) or as a separate micelle (VIPER + NPSTING). Tumor volume and survival were monitored throughout the study. While VIPER alone modestly slowed tumor growth, its combination with polySTING or NPSTING significantly enhanced therapeutic efficacy. Notably, the free STING agonist failed to improve survival despite eliciting T cell responses, underscoring the importance of pharmacokinetics and targeted delivery. Mice treated with

VIPER-co-NPSTING showed the greatest tumor suppression and survival benefit, highlighting the critical role of co-delivering both antigen and adjuvant within the same nanoparticle. As it pertains to my project, the next step is to test if this co-delivery of STING with VIPER would cause suboptimal effects due to pH changes induced to targeted cells.

Materials and Methods

Synthesis of Polymers

The synthesis pathway for the STING Agonist-3 prodrug monomer is summarized in Figure 1. Using the polymerizable mono-2-(methacryloyloxy)ethyl succinate (SMA) moiety, the prodrug monomer was synthesized by incorporating the cathepsin-B cleavable Val-Ala (VA) linker with a self-immolative para-aminobenzyl alcohol (PABA) moiety to yield SMA-Val-Ala-PABA-STING Agonist-3 (SVA-PAB-STING). The prodrug monomer product was characterized using 1 H NMR and mass spectrometry. The targeted polymer prodrug “drugamer” polySTING was then synthesized by copolymerizing SVA-PAB-STING with mannose ethyl methacrylate (ManEMA). We confirmed by dynamic light scattering that polySTING is highly soluble in aqueous solutions as unimers of up to 200 mg/mL in PBS. PolySTING is thus designed for internalization by receptor-mediated endocytosis in CD206+ cells, followed by endosomal cathepsin cleavage and release of the membrane permeable diABZI-type STING Agonist-3 that can activate the cytosolic STING protein in these antigen presenting cells.

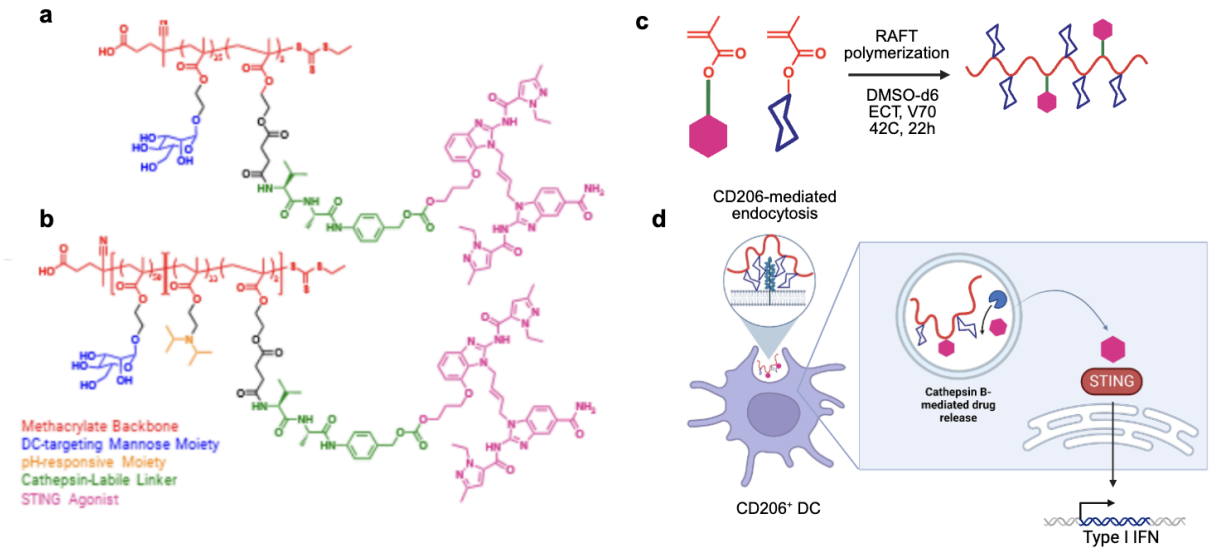

Figure 1. Design of a STING polymeric prodrug. (a-b) Chemical structures of polySTING and NPSTING with NMR-determined degrees of polymerization indicated, respectively. (c) Schematic of synthesis by RAFT polymerization. (d)

Schematic of STING polymer uptake by DCs, endosomal prodrug cleavage and agonist release, and STING activation in DCs.

For the synthesis of NPSTING, ManEMA was combined with ECT, ABCVA (ECT:ManEMA = 1:44.4, ECT:ABCVA = 1:20) in dry DMSO (2.5 wt% monomer), purged with argon for 30 minutes, and reacted at 70°C for 4h with vigorous stirring. The mannose CTA (ManCTA) was purified by 3x precipitation in 1:1 (v/v) acetone and diethyl ether, dissolving in DMF in-between, and dried *in vacuo* for 2 days. To a 5 mL round-bottom flask with a stir bar, ManCTA, SMA-VA-STING, DIPAMA and V70 (ManCTA:SVA-VA-STING:DIPAMA:V70 = 1:5:33:0.25) was added as well as anhydrous NMP as a solvent (20 wt% monomer). The solution was stirred until all solids were fully dissolved. 8 µl of DMF was added (~1% v/v NMP) as an internal standard. A 20 µl aliquot of the reaction mixture was taken as a reference for conversion NMR. The flask was sealed with a septum and sparged with argon gas for 30 minutes. The mixture was then allowed to react by stirring at 40°C for 20 hours, before being quenched by introduction of air and chilling via an ice bath. The polymer was purified via dialysis in DMSO for 3 days (2 solvent changes each day), and in cold water for 4 days (2-3 solvent changes each day) before lyophilization to yield a fluffy white powder (150 mg, 90% conversion, 87% yield from purification).

Phase 1: Preliminary Tube Protocol for Endosomal pH

DC2.4 cells were cultured in RPMI supplemented with 10% heat-inactivated FBS and 1% Penicillin-Streptomycin (P/S). Hela cells were cultured in DMEM supplemented with 10% FBS and 1% P/S. Cells were incubated at 37°C and 5% CO2. Fluorescein isothiocyanate (FITC)- and Alexa Fluor 647-labeled 10,000 MW dextrans were dissolved at concentrations of 10 mg/mL and 5 mg/mL, respectively. Cells were counted, and aliquots of 3×10^6 cells were reserved for pH measurement at multiple time points and 2×10^6 cells for the standard curve.

For the pH standard curve, cells were resuspended in 75 µL of prewarmed conditioned complete medium containing 1 mg/mL FITC-dextran and 0.5 mg/mL Alexa-647-dextran, and pulsed in a 37 °C water bath for 10 minutes. To halt internalization, 1 mL of ice-cold PBS supplemented with 1% BSA was added, followed by five washes with the same buffer to remove non-internalized dextran. Cells were divided into four 1.5 mL tubes, each resuspended in a buffer of defined pH containing 0.1% Triton X-100 to equilibrate intracellular pH with the external buffer. After gentle mixing, bead-associated fluorescence was immediately analyzed by flow cytometry.

For time course measurements, cells were resuspended in 112.5 µL of prewarmed conditioned complete medium containing 1 mg/mL FITC-dextran and 0.5 mg/mL Alexa-647-dextran and pulsed at 37 °C for 10 minutes. The reaction was stopped using 1 mL of ice-cold PBS with 1% BSA, followed by five washes to remove extracellular dextran. Cells were then resuspended in 1 mL of prewarmed conditioned complete medium and incubated at 37 °C for various chase time points prior to analysis

with flow cytometry. Data analysis was performed using FlowJo software (FlowJo, LLC), with serial gating.

Phase 2: Optimized Tube Protocol for Endosomal pH

Cells were cultured as previously described. Fluorescein isothiocyanate (FITC)- and Alexa Fluor 647-labeled 10,000 MW dextrans were dissolved at concentrations of 10 mg/mL and 5 mg/mL, respectively. Cells were counted, and aliquots of 6×10^6 cells were reserved for pH measurement at multiple time points and 2×10^6 cells for the standard curve.

For the pH standard curve, cells were resuspended in 75 µL of prewarmed conditioned complete medium containing 1 mg/mL FITC-dextran and 0.5 mg/mL Alexa-647-dextran, and pulsed in a 37 °C water bath for 10 minutes. To halt internalization, 1 mL of ice-cold PBS supplemented with 1% BSA and 1% heparan sulfate was added, followed by three washes with the same buffer to remove non-internalized dextran. Cells were divided into four 1.5 mL tubes, each resuspended in a buffer of defined pH containing 0.1% Nigericin and Valinomycin (X-1000) to equilibrate intracellular pH with the external buffer. After gentle mixing and incubation at 37 °C for at least 5 minutes, bead-associated fluorescence was immediately analyzed by flow cytometry.

For time course measurements, cells were resuspended in 112.5 µL of prewarmed conditioned complete medium containing 1 mg/mL FITC-dextran and 0.5 mg/mL Alexa-647-dextran and pulsed at 37 °C for 10 minutes. The reaction was stopped using 1 mL of ice-cold PBS with 1% BSA and 1% heparan sulfate, followed by three washes to remove extracellular dextran. Cells were then resuspended in 1 mL of prewarmed conditioned complete medium and incubated at 37 °C for various chase time points prior to analysis with flow cytometry.

Phase 3: Finalized Protocol for DC Endosomal pH with STING Variant Co-Treatment

DC2.4 cells were seeded into U-bottom TC-treated 96 well plates at 50,000 cells per well in 80 µL of complete RPMI medium, and incubated at 37°C and 5% CO2 overnight. 10X Vaccine formulations for free, poly and NPSTING were created at 200 ug/mL in dPBS and sterile filtered using a 0.22 micron filter. In parallel, a 10X dextran loading mixture was prepared containing 20 µL of 10 mg/mL FITC-dextran, 20 µL of 5 mg/mL Alexa Fluor 647-dextran, and 960 µL of complete RPMI medium. At designated time points prior to analysis (5, 10, 20, 30, 60, 90, and 120 minutes), 10 µL of the 10X dextran mixture was added to each corresponding well, along with 10 µL of either a 10X vaccine formulation or PBS control. For standard curve generation, 10 µL of the 10X dextran mixture and 10 µL of PBS were added to the respective wells 60 minutes prior to analysis. Plates were incubated at 37 °C until the final time point.

Following incubation, cells were washed three times with ice-cold PBS containing 1% BSA and 1% heparan sulfate (PBSA-HS) to remove non-internalized dextran. Cells

were then resuspended in 200 µL of either PBS (for analysis) or pH calibration buffers supplemented with 0.2 µL of Nigericin/Valinomycin (V/N) membrane permeabilization cocktail. Samples were transferred to flat-bottom 96-well plates and incubated at 37 °C for 5 minutes before flow cytometric analysis.

Results and discussions

Assay Development

Following the analysis of my first and second assay trial, the calibration curve was shown to be very close to linear as expected, with an increase in the intensity ratio of FITC/A647 correlated with an increase in pH. Using this calibration curve to assign pH values to FITC/A647 intensity values recovered from the cells incubated for chase time points, there was seemingly no change in acidity. In fact, there seemed to be a stagnant plateau at pH 4.5 for all time-points. This is not the trend expected, since literature tells us that over time, endosomal maturation into a lysosome results in lower pH values due to proton trafficking into the vesicle [19]. Upon looking at the flow cytometry plots, one of which is shown in Figure 2, we can see that instead of one distinct population of cells and another of cell debris, there is one large cluster of data points. This likely indicated that cell viability was low when samples were run on the flow cytometer. The most reasonable cause of this would be the membrane permeabilizing agent Triton X-100, which at high enough concentrations is known to lyse cells instead of permeabilizing them [20]. Additionally, another possibility could be that since the protocol calls for five washes, in the time it takes to complete these manual washes, all the endosomes might have matured, which is why we only see one exceptionally acidic value.

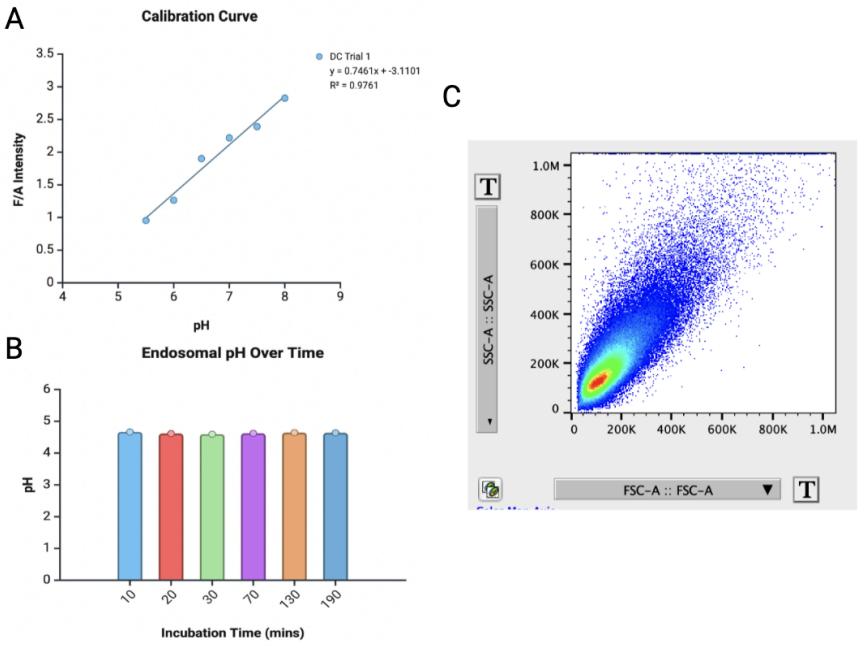

Figure 2. Results from tube trial 1 with DCs. (a) Calibration curve generated from analyzing membrane permeabilized cells suspended in various pH buffers of known value. (b) pH values of time point incubated cells resulting from calibration curve. (c) Flow cytometry plot of 70 minute incubation generated using FlowJo software.

After this assay was run three times at N=2 and a stagnant pH of 4.5 with potential cell death was observed each time, a switch was made to a valinomycin and nigericin cocktail instead of triton X-100 to permeabilize the cells in a gentler way. Additionally, instead of 5 washes, the cells were washed 3 times to reduce time in between dextran uptake and analysis. In this wash buffer, heparan sulfate was also added in order to serve as a competitive inhibitor of the dextrans, blocking non-specific binding sites on the cell surface and washing away non-internalized dextrans.

A switch was made to using HeLa cells to further optimize this assay in a robust cell line before making a return to DCs, because they are a non-standard cell line.

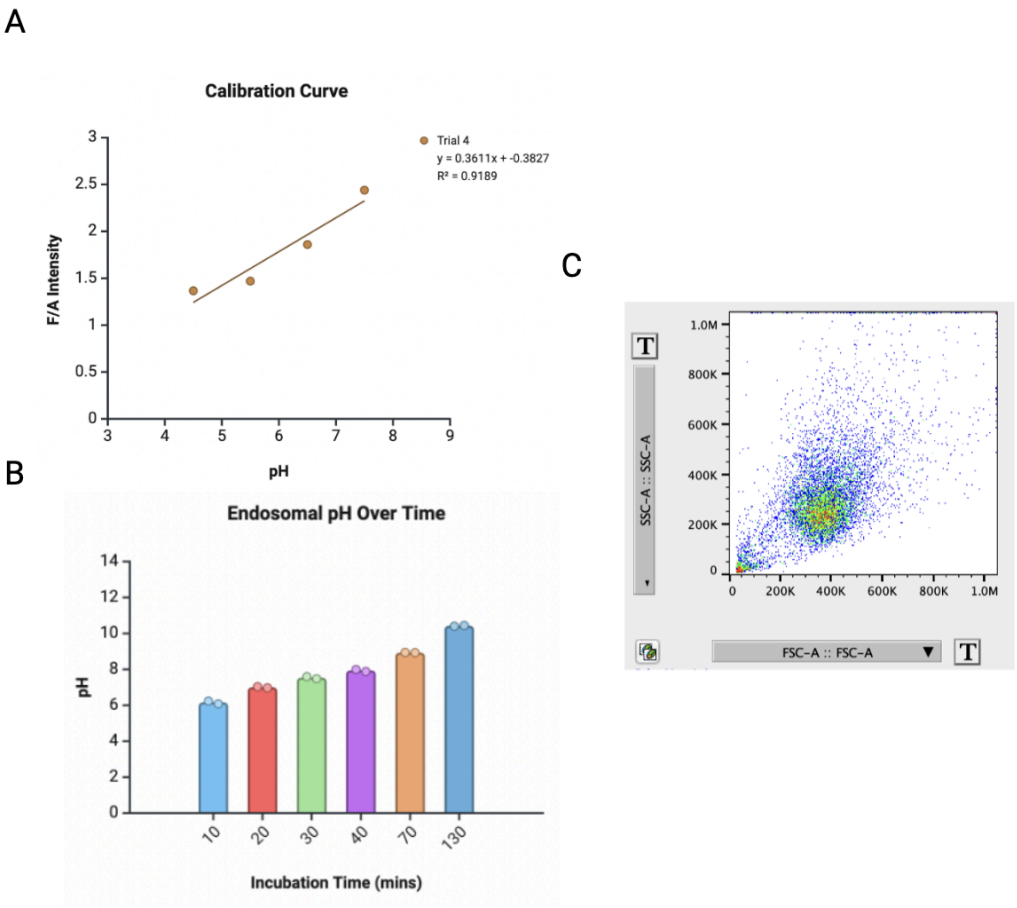

Figure 3. Results from tube trial 4 with HeLa cells. (a) Calibration curve generated from analyzing membrane permeabilized cells suspended in various pH buffers of known value using V/N cocktail. (b) pH values of time point incubated cells resulting from calibration curve. (c) Flow cytometry plot of 70 minute incubation generated using FlowJo software.

Following the analysis of the data from the newly revised protocol in HeLa cells, much higher cell viability was observed, as indicated by the two distinct populations in the flow cytometry plot. The population with lower forward scatter and side scatter has smaller size and lower granularity, and is therefore most likely cell debris. Therefore, the other population was gated on for analysis, because it is thought to represent the live HeLa cells. From the analysis, we see a nice transition in pH values, but instead of seeing acidification we see the exact opposite. In fact, if the values were mirrored over pH 7, they would encapsulate the theoretical values commonly used in literature for endosomal pH. Looking at the raw numerical fluorescence data, it was observed that over time A647 fluorescence was being quenched at a much higher rate than FITC, leading to the high values in pH that we observe. Since both FITC and A647 fluorescence were decreasing when A647 was theorized to be stable, this points to

exocytosis as the culprit for the alkalinization we observe here. Though this protocol fixed the viability issues encountered earlier, it inadvertently introduced a new issue with the use of HeLa cells. Thus, this validates our switch back to DCs.

Olden et al. describe the use of a ratiometric method for intracellular pH compartment measurement by incubating T cells in 48 well plates instead of tubes [21]. This would use less cell and dye concentration, as well as be easier to run with higher throughput. Thus, the switch was made to incubate the cells in 48 well plates with the dextrans, and then wash them all at once before flow cytometric analysis. In the first trial using the plates, the calibration curve cells were incubated in the dextrans for 10 minutes, while the experimental cells were incubated at various chase time points prior to washing and analysis.

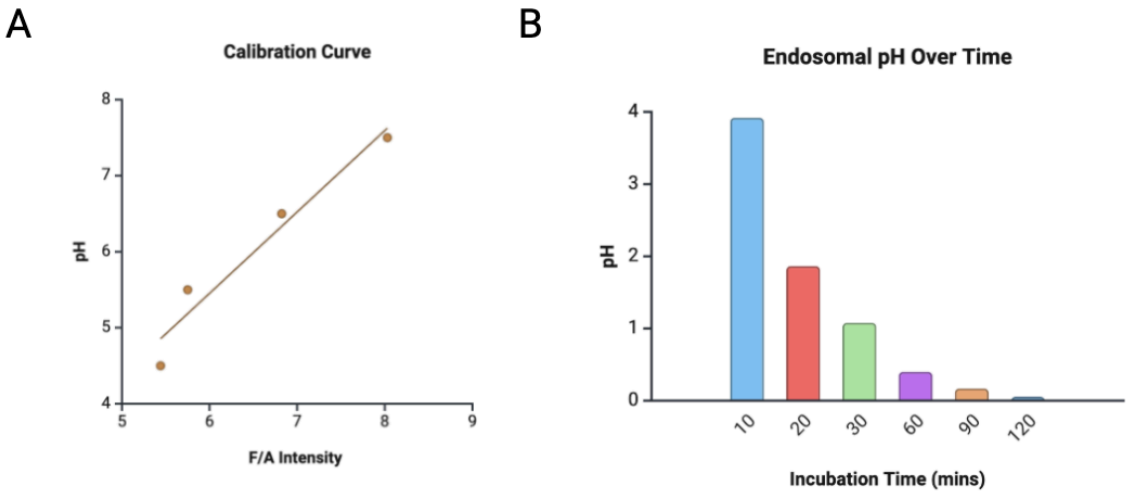

Figure 4. Results from plate trial 1 with DCs incubated in 48 well plates. (a) Calibration curve generated from analyzing membrane permeabilized cells suspended in various pH buffers of known value using V/N cocktail. (b) pH values of time point incubated cells resulting from calibration curve.

The resulting pH data from this trial shown in Figure 4 panel B depicts a nice acidic trend over time, which is what was expected from the data. The actual values of the pH, however, were not correct and the transition from the 10 minute to 120 minute incubation was too steep to be believable. Taking a look at the raw numerical fluorescent data for each of the fluorophores separately showed me that the calibration curve cells had internalized far fewer A647 conjugated dextrans than the time point cells. This was skewing the data to present the endosomes as more acidic than they actually are. As a way to combat this, the next trial had the calibration curve cells incubated at 60 minutes with the dextrans before analysis, since this time point is in the middle of the most extreme groups measured in the experimental groups.

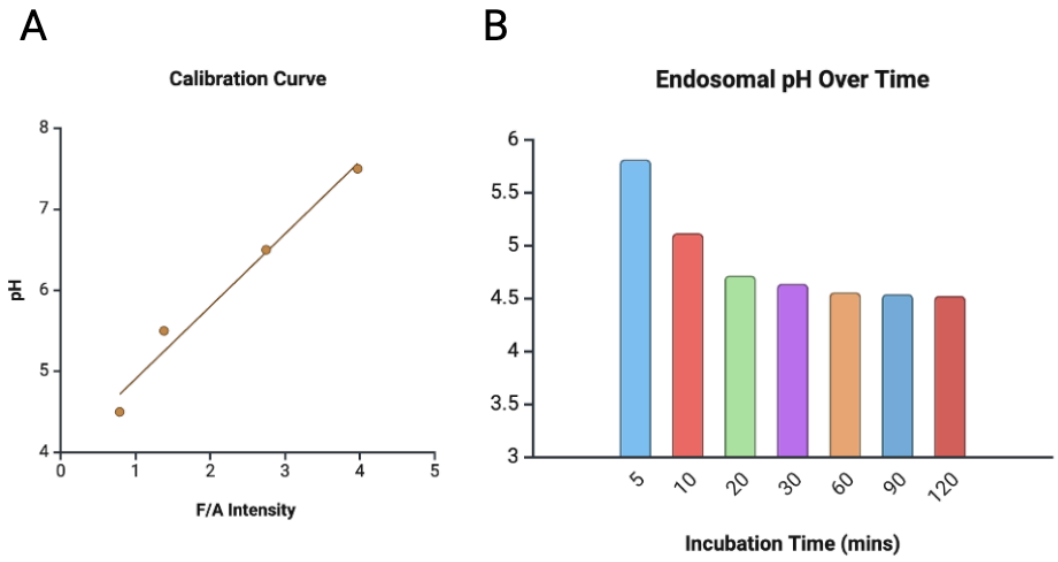

Figure 5. Results from plate trial 2 with DCs incubated in 48 well plates. (a) Calibration curve generated from analyzing membrane permeabilized cells suspended in various pH buffers of known value using V/N cocktail. (b) pH values of time point incubated cells resulting from calibration curve.

The trend we see in endosomal pH occurring in Figure 5 is exactly what was expected from dendritic cells, where there is a steady increase in acidity over time due to endosomal maturation. Additionally, the actual values of the pHs look to be biologically relevant to what is generally expected of endosomes of other cell types, further validating that this assay has worked [22]. Building upon the success of these findings, we can increase the throughput of this assay to allow for the comparison of different treatment groups and increase the sample size to bolster statistical power and enhance the reliability of results. The natural way to do this would be to replicate the plates by running multiple in parallel; however, due to the nature of flow cytometry this is not easily achievable since each sample must be processed one at a time, which skews the time in between dextran uptake between samples. Thus, I decided to scale the assay to a 96 well plate format to allow for the measurement of multiple experimental conditions at a time with a higher throughput on the same plate. This change required scaling down the concentrations of cells, dyes and dextrans in a 1:3 ratio to account for the change in volume between the 48 well plates and 96 well plates.

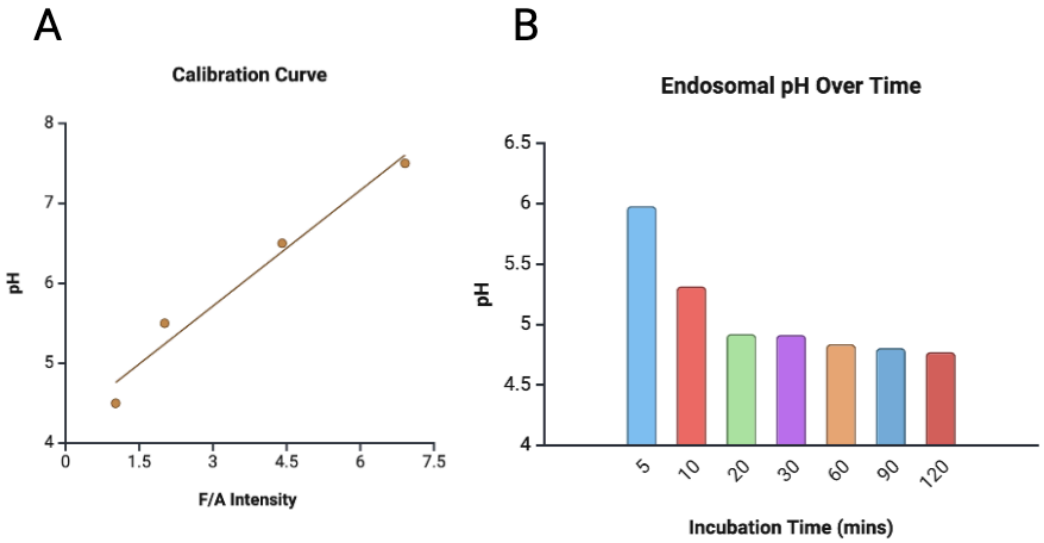

Figure 6. Results from plate trial 3 with DCs incubated in 96 well plates. (a) Calibration curve generated from analyzing membrane permeabilized cells suspended in various pH buffers of known value using V/N cocktail. (b) pH values of time point incubated cells resulting from calibration curve.

Following the analysis of the data from the newly revised protocol in 96 well plates, we see data with resulting endosomal pH values that closely match the results of trial 2 in 48 well plates. This is a clear indication that the values we are measuring are biologically accurate and that the scaling to higher throughput methods worked. This validates moving forward to testing the effects of variant STING treatment on endosomal pH using this optimized protocol.

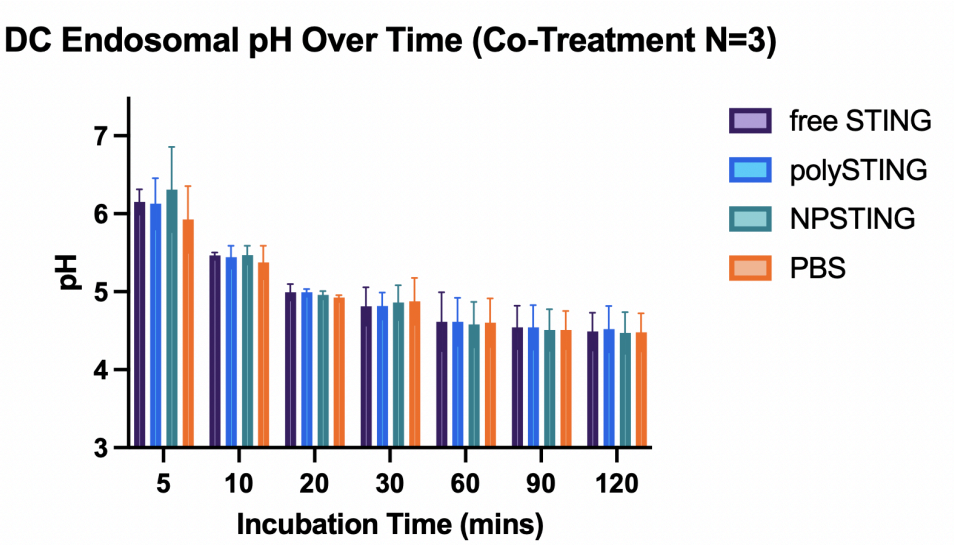

Figure 7. Results from STING variant co-treatment with dextrans on DCs in 96 well plates (N=3)

Figure 7 presents the results of endosomal pH measurements in DCs co-treated with various STING agonist formulations. Across all time points, the acidification profiles for free STING, polySTING, and NPSTING groups followed a similar trend to the PBS control, with a progressive decline in pH indicative of typical endosomal maturation. Notably, while the general acidification trajectory was preserved, a modest delay in acidification was observed in the NPSTING group relative to PBS, especially at earlier time points (5 - 30 minutes). However, these shifts were not statistically significant and did not reflect a complete inhibition or reversal of acidification.

These results suggest that immediate co-treatment with STING agonists does not drastically disrupt endosomal pH homeostasis. This finding is encouraging for STING/VIPER combination therapy, as it indicates that simultaneous delivery is unlikely to interfere with VIPER's pH-dependent membrane escape at the point of cellular uptake. However, subtle differences in acidification kinetics hint at the possibility that STING-induced signaling may require more time to fully impact vesicular behavior.

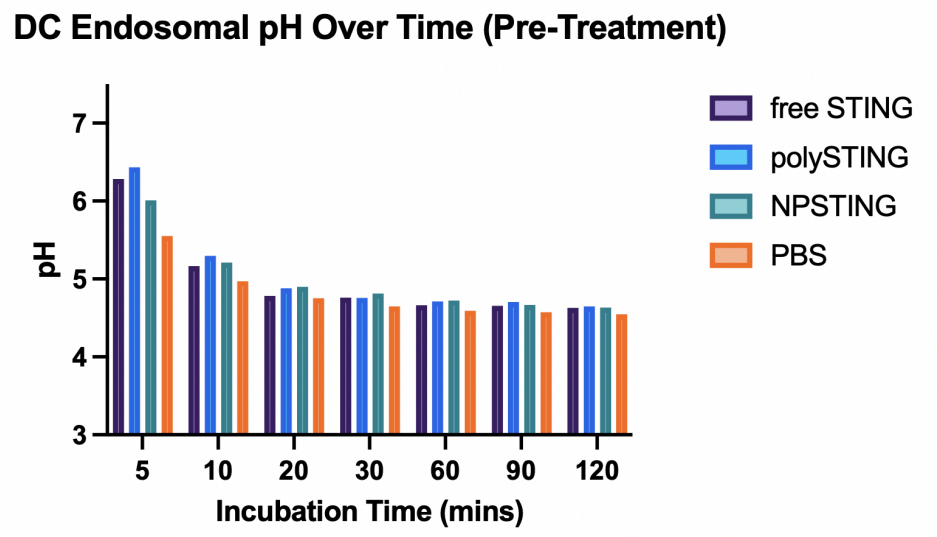

Figure 8. Results from STING variant 30-minute pre-treatment with dextrans on DCs in 96 well plates

Figure 8 shows the results of a 30-minute pretreatment of DCs with STING agonists prior to dextran loading and endosomal pH analysis. Unlike the co-treatment condition, pretreatment enabled STING-mediated signaling events such as IFN production, metabolic reprogramming, or endosomal remodeling to initiate before pH-sensitive uptake occurred. Under these conditions, a more noticeable delay in acidification was observed, especially in the polySTING-treated group. The polySTING condition maintained a higher endosomal pH across the 120-minute window compared to PBS, although it is still a very minor difference.

These findings suggest that prior activation of STING signaling can very minorly influence vesicle maturation or trafficking pathways, potentially by modifying endosomal proton transport or altering membrane dynamics. This has important implications for antigen delivery systems like VIPER that rely on acidic pH for cargo release. If STING activation precedes antigen delivery, there may be diminished endosomal escape efficiency, potentially reducing therapeutic efficacy. Therefore, treatment timing should be carefully considered in combination therapies using pH-responsive nanocarriers and immunostimulatory adjuvants.

Future Work

To build upon the findings of this project, several next steps can be proposed. The immediate next step would be to complete triplicate flow cytometry runs of the 20 minute STING pre-treatment in order to compare endosomal pH modulation across different groups using one-way ANOVA to assess statistical significance. Additionally, we can find optimal STING pre-treatment timing by exploring the effects of different pre-treatment durations (e.g., 15, 30, 60 minutes) on endosomal pH prior to dextran exposure to assess temporal dynamics of STING-mediated pH modulation and endocytosis. We can also implement an alternative fluorescence-based method (e.g., confocal microscopy or high-content imaging) to validate pH measurements and spatially resolve intracellular compartments, strengthening confidence in the assay's output using an orthogonal fluorescence measurement method. Additionally, an avenue to possibly go down would be to test any synergistic effects from having a multi-adjuvant vaccine. Specifically, toll-like receptor (TLR) 9 activation has been shown to aid in activation of the cancer killing cascade [29]. Thus, we can see if combining TLR9 agonists with polySTING will induce a more potent anti-cancer response than either treatments alone. We can also assess the impact of variant STING treatment on VIPER release kinetics in DCs by performing mechanistic studies on how STING-induced pH changes influence VIPER nanoparticle disassembly and melittin-mediated endosomal escape, using various fluorescence dequenching or release assays. These future directions will deepen our understanding of the interplay between immune activation and intracellular drug delivery kinetics, and contribute to the rational design of next-generation cancer vaccines with improved safety and efficacy.

Impact

The impact of this work has broad global implications. Enhancing tumor-specific immune responses through targeting STING agonists to DCs could dramatically improve the efficacy of immunotherapy for solid tumors. This will lead to better cancer treatment outcomes and improved patient quality of life. This work is extremely relevant to population health due to the fact that cancer virtually affects the entire population in some way or another, transcending socio-cultural boundaries in the process. Unfortunately, treatments for cancer such as chemotherapy can be extremely expensive and cause a plethora of unpleasant side effects. Having a simple and effective vaccine would lessen the burden of the cost and be less invasive, leading to increased availability regardless of socioeconomic status.

From an environmental perspective, the polymer nanomedicine approach used in this work reduces the amount of small molecule drugs needed for effective treatment, which cuts down on chemical waste. Furthermore, the improved specificity of the drug delivery to target tissues avoids the loss of drug through unspecific distribution and accumulation in healthy tissues, further reducing the amount of drug needed. In a societal context, making cancer treatment more accessible and less resource-intensive overall will have a positive impact on communities and families dealing with cancer.

Acknowledgements

This work was supported by the U.S. National Institutes of Health and the University of Washington Department of Bioengineering. I am beyond grateful to Dr. Kefan Song, Dr. Dinh Chuong Nguyen, Yonghui Wang, and Dr. Suzie Pun for their unwavering support over the course of my time working on this project and in the Pun lab as a whole. As a rising sophomore at the University of Washington, Drs. Pun and Song took me under their wing and transformed me from someone who was intimidated by a micropipette to being confident in conducting experiments, developing protocols, and co-authoring multiple publications. I am eternally grateful for their belief in me.

I would also like to thank Dr. Christopher Neils for his support throughout my time in the Bioengineering department. It is with his guidance and teaching in the Bioengineering core curriculum that I can now call myself a bioengineer.

References

[1] R. L. Siegel, K. D. Miller, H. E. Fuchs, and A. Jemal, “Cancer statistics, 2022,” *CA: A Cancer Journal for Clinicians*, vol. 72, no. 1, pp. 7–33, 2022.

[2] *Charted: What America-and the rest of the world-spends on cancer*. [Online]. Available: https://www.advisory.com/daily-briefing/2022/06/02/cancer-care#:~:text=%22The%20U.S.%20is%20spending%20over,Clinical%20Scholars%20Program%20at%20Yale. [Accessed: 07-May-2023].

[3] Z. Hu, P. A. Ott, and C. J. Wu, “Towards personalized, tumour-specific, therapeutic vaccines for cancer,” *Nature Reviews Immunology*, vol. 18, no. 3, pp. 168–182, 2017.

[4] W. Liu, H. Tang, L. Li, X. Wang, Z. Yu, and J. Li, “Peptide based therapeutic cancer vaccine: Current trends in clinical application,” *Cell Proliferation*, vol. 54, no. 5, 2021.

[5] A. J. Convertine, D. S. W. Benoit, C. L. Duvall, K. S. Hoffman, and P. S. Stayton, “pH-Responsive Polymer Micelles for Intracellular Delivery of Hydrophobic Chemotherapeutic Agents,” Journal of Controlled Release, vol. 133, no. 3, pp. 221–229, 2009.

[6] “Mission and goals,” *National Institutes of Health*, 27-Jul-2017. [Online]. Available: https://www.nih.gov/about-nih/what-we-do/mission-goals. [Accessed: 07-May-2023].

[7] A. K. Singh, M. Praharaj, K. A. Lombardo, T. Yoshida, A. Matoso, A. S. Baras, L. Zhao, G. Srikrishna, J. Huang, P. Prasad, J. D. Powell, M. Kates, D. McConkey, D. M. Pardoll, W. R. Bishai, and T. J. Bivalacqua, “Re-engineered BCG overexpressing cyclic di-AMP augments trained immunity and exhibits improved efficacy against bladder cancer,” *Nature Communications*, vol. 13, no. 1, 2022.

[8] J. M. Ramanjulu, G. S. Pesiridis, J. Yang, N. Concha, R. Singhaus, S.-Y. Zhang, J.-L. Tran, P. Moore, S. Lehmann, H. C. Eberl, M. Muelbaier, J. L. Schneck, J. Clemens, M. Adam, J. Mehlmann, J. Romano, A. Morales, J. Kang, L. Leister, T. L. Graybill, A. K. Charnley, G. Ye, N. Nevins, K. Behnia, A. I. Wolf, V. Kasparcova, K. Nurse, L. Wang, A. C. Puhl, Y. Li, M. Klein, C. B. Hopson, J. Guss, M. Bantscheff, G. Bergamini, M. A. Reilly, Y. Lian, K. J. Duffy, J. Adams, K. P. Foley, P. J. Gough, R. W. Marquis, J. Smothers, A. Hoos, and J. Bertin, “Design of amidobenzimidazole sting receptor agonists with systemic activity,” *Nature*, vol. 564, no. 7736, pp. 439–443, 2018.

[9] M. Luo, H. Wang, Z. Wang, H. Cai, Z. Lu, Y. Li, M. Du, G. Huang, C. Wang, X. Chen, M. R. Porembka, J. Lea, A. E. Frankel, Y.-X. Fu, Z. J. Chen, and J. Gao, “A sting-activating nanovaccine for cancer immunotherapy,” *Nature Nanotechnology*, vol. 12, no. 7, pp. 648–654, 2017.

[10] Q. Wang, J. S. Bergholz, L. Ding, Z. Lin, S. K. Kabraji, M. E. Hughes, X. He, S. Xie, T. Jiang, W. Wang, J. J. Zoeller, H.-J. Kim, T. M. Roberts, P. A. Konstantinopoulos, U. A. Matulonis, D. A. Dillon, E. P. Winer, N. U. Lin, and J. J. Zhao, “Sting agonism reprograms tumor-associated macrophages and overcomes resistance to PARP inhibition in BRCA1-deficient models of breast cancer,” *Nature Communications*, vol. 13, no. 1, 2022.

[11] T. Ohkuri, A. Kosaka, T. Nagato, and H. Kobayashi, “Effects of sting stimulation on macrophages: Sting agonists polarize into ‘classically’ or ‘alternatively’ activated macrophages?,” *Human Vaccines & Immunotherapeutics*, vol. 14, no. 2, pp. 285–287, 2017.

[12] Y.-tong Wu, Y. Fang, Q. Wei, H. Shi, H. Tan, Y. Deng, Z. Zeng, J. Qiu, C. Chen, L. Sun, and Z. J. Chen, “Tumor-targeted delivery of a sting agonist improvescancer immunotherapy,” *Proceedings of the National Academy of Sciences*, vol. 119, no. 49, 2022.

[13] J. M. Jaynes, R. Sable, M. Ronzetti, W. Bautista, Z. Knotts, A. Abisoye-Ogunniyan, D. Li, R. Calvo, M. Dashnyam, A. Singh, T. Guerin, J. White, S. Ravichandran, P. Kumar, K. Talsania, V. Chen, A. Ghebremedhin, B. Karanam, A. Bin Salam, R. Amin, T. Odzorig, T. Aiken, V. Nguyen, Y. Bian, J. C. Zarif, A. E. de Groot, M. Mehta, L. Fan, X. Hu, A. Simeonov, N. Pate, M. Abu-Asab, M. Ferrer, N. Southall, C.-Y. Ock, Y. Zhao, H. Lopez, S. Kozlov, N. de Val, C. C. Yates, B. Baljinnyam, J. Marugan, and U. Rudloff, “Mannose receptor (CD206) activation in tumor-associated macrophages enhances adaptive and innate antitumor immune responses,” *Science Translational Medicine*, vol. 12, no. 530, 2020.

[14] J. Ye, Y. Yang, W. Dong, Y. Gao, Y. Meng, H. Wang, L. Li, J. Jin, M. Ji, X. Xia, X. Chen, Y. Jin, and Y. Liu, “drug-free mannosylated liposomes inhibit tumor growth by promoting the polarization of tumor-associated macrophages,” *International Journal of Nanomedicine*, vol. Volume 14, pp. 3203–3220, 2019.

[15] C. Pantelidou, O. Sonzogni, M. De Oliveria Taveira, A. K. Mehta, A. Kothari, D. Wang, T. Visal, M. K. Li, J. Pinto, J. A. Castrillon, E. M. Cheney, P. Bouwman, J. Jonkers, S. Rottenberg, J. L. Guerriero, G. M. Wulf, and G. I. Shapiro, “PARP inhibitor efficacy depends on CD8+ T-cell recruitment via intratumoral sting pathway activation in BRCA-deficient models of triple-negative breast cancer,” *Cancer Discovery*, vol. 9, no. 6, pp. 722–737, 2019.

[16] Y. Da, Y. Liu, Y. Hu, W. Liu, J. Ma, N. Lu, C. Zhang, and C. Zhang, “Sting agonist CGAMP enhances anti-tumor activity of car-NK cells against pancreatic cancer,” *OncoImmunology*, vol. 11, no. 1, 2022.

[17] C. Zhang, G. Shang, X. Gui, X. Zhang, B. X. Bai, and Z. J. Chen, “Structural basis of STING binding with and phosphorylation by TBK1,” Nature, vol. 567, no. 7748, pp. 394–398, 2019.

[18] F.-Y. Su, S. Srinivasan, B. Lee, J. Chen, A. J. Convertine, T. E. West, D. M. Ratner, S. J. Skerrett, and P. S. Stayton, “Macrophage-targeted drugamers with enzyme-cleavable linkers deliver high intracellular drug dosing and sustained drug pharmacokinetics against alveolar pulmonary infections,” *Journal of Controlled Release*, vol. 287, pp. 1–11, 2018.

[19] I. Mellman, R. Fuchs, and A. Helenius, “Acidification of the endocytic and exocytic pathways,” Annual Review of Biochemistry, vol. 55, pp. 663–700, 1986.

[20] J. M. Neugebauer, “Detergents: An Overview,” in Methods in Enzymology, vol. 182, pp. 239–253, Academic Press, 1990.

[21] B. R. Olden, Y. Cheng, J. L. Yu, and S. H. Pun, “Cationic polymers for non-viral gene delivery to human T cells,” Journal of Controlled Release, vol. 282, pp. 120–130, 2018.

[22] D. Tapia, M. Jiménez-Reyes, J. Vargas, et al., “Endosomal pH profiling in dendritic cells reveals distinct trafficking regulation for processing antigens,” Scientific Reports, vol. 7, no. 1, 2017.